SEARCH FOR LEPTON FLAVOUR VIOLATION WITH THE $\mu^+ \to e^+\gamma$ DECAY: FIRST RESULTS FROM THE MEG EXPERIMENT

Giovanni Signorelli*

INFN Sezione di Pisa, Largo Bruno Pontecorvo 3,
I-56127 Pisa, Italy
E-mail: giovanni.signorelli@pi.infn.it

The MEG experiment aims at testing the lepton-flavour symmetry, present in the Standard Model, by searching for the $\mu^+ \to e^+\gamma$ decay with a sensitivity of a few $\times 10^{-13}$, two orders of magnitude better than the present experimental limit. Novel detectors were developed for this measurement as well as multiple and redundant calibrations which are mandatory to constantly monitor the performance and possible drifts in the apparatus. The experiment had a start-up physics run in the last three months of 2008 at reduced acceptance. From the analysis of the first data a limit on the branching ratio of $BR(\mu^+ \to e^+\gamma) < 2.8 \times 10^{-11}$ was obtained, which is about a factor of two larger than the present experimental limit set by the previous experiment. The experiment finished a second short run in 2009 and is scheduled to take data in 2010 and 2011 to reach its full sensitivity.

Keywords: Muon decay; Lepton Flavour Violation; MEG.

1. Introduction

The MEG experiment, hosted by the Paul Scherrer Institut in Villigen (Switzerland) is designed and built by an international collaboration made of physicists from Italy, Japan, Russia, Switzerland and the United States and aims at measuring the branching ratio $BR(\mu^+ \to e^+\gamma/\mu \to e\nu\bar{\nu})$ with unprecedented sensitivity.[1]

The $\mu^+ \to e^+\gamma$ decay is forbidden in the Standard Model of elementary particles (SM) by the fact that the neutrinos of the three families are massless and degenerate. With the introduction of neutrino masses and mixings in the model, the $\mu^+ \to e^+\gamma$

*On behalf of the MEG collaboration: J. Adam, X. Bai, A. Baldini, E. Baracchini, A. Barchiesi, C. Bemporad, G. Boca, P. W. Cattaneo, G. Cavoto, G. Cecchet, F. Cei, C. Cerri, A. De Bari, M. De Gerone, T. Doke, S. Dussoni, J. Egger, L. Galli, G. Gallucci, F. Gatti, B. Golden, M. Grassi, D. N. Grigoriev, T. Haruyama, M. Hildebrandt, Y. Hisamatsu, F. Ignatov, T. Iwamoto, D. Kaneko, P.-R. Kettle, B. I. Khazin, O. Kiselev, A. Korenchenko, N. Kravchuk, A. Maki, S. Mihara, W. Molzon, T. Mori, D. Mzavia, H. Natori, R. Nardò, D. Nicolò, H. Nishiguchi, Y. Nishimura, W. Ootani, M. Panareo, A. Papa, R. Pazzi, G. Piredda, A. Popov, F. Renga, S. Ritt, M. Rossella, R. Sawada, M. Schneebeli, F. Sergiampietri, G. Signorelli, S. Suzuki, C. Topchyan, V. Tumakov, Y. Uchiyama, R. Valle, C. Voena, F. Xiao, S. Yamada, A. Yamamoto, S. Yamashita, Yu. V. Yudin, D. Zanello (Dubna, Genova, KEK, Lecce, Novisibirsk, Pavia, Pisa, PSI, Roma I, Tokyo, UCI, Waseda).

decay is radiatively induced, but at a negligible level, since the muon neutrino has to oscillate into an elecron neutrino during a W-boson's lifetime, resulting in a probability for this process of $\sim 10^{-54}$.

It is generally believed that the SM is just a low energy approximation of a more fundamental theory, and in all its extensions the rate for the $\mu^+ \to e^+\gamma$ process is enhanced by mixings that are naturally present in the high energy sector of these theories, since many more particle can circulate in the loop turning the initial muon flavour into an electron final state.

Predictions can be made for the decay rate that depend to some extent on the kind of theory (supersymmetric grand-unification theory, extra-dimensions, heavy right-handed neutrinos...) but are generally in the range of $BR(\mu^+ \to e^+\gamma) \approx 10^{-12} \div 10^{-14}$.[2–4]

An experiment that is able to explore such range of probabilities has therefore the potential to discover the physics beyond the SM or pose serious constraints to its possible extensions.

1.1. *Connections with other branches of particle physics*

The search for this rare decay has many connections with other branches of physics, that may be more familiar to the reader. We just want to give here three examples of such links.

(a) The quest for the $\mu^+ \to e^+\gamma$ decay is a way to search for physics beyond the SM which is complementary to the search for new particles performed at the high energy frontier (*e.g.* at the LHC). The small terms in the model Lagrangian which are suppressed by powers of E/M, where E is the energy scale of the process and M is the new physics mass scale, are investigated not by increasing the energy (and enhancing the process) but performing a precision experiment.

(b) The estabilished phenomenology of neutrino oscillations[5] implies that the neutral leptons do mix. It is natural to believe that such mixing is transferred to the charge leptons through their common high energy partners. Models exist in which this mixing is maximal (PMNS-like, or similar to the neutrino mixing) or minimal (CKM-like, similar to the quark mixing). Depending on the case the observation or exclusion of the $\mu^+ \to e^+\gamma$ process can shed light on the nature of such mixing.[6]

(c) The experimental measurement of the anomaly of the muon magnetic moment (a_μ) differs by the SM-prediction by 3.4 σs.[7] The Feynman diagrams that describe the contributions to a_μ and $\mu^+ \to e^+\gamma$ are the same, once the outgoing muon leg is replaced by an electron: the muon anomaly is related to the diagonal part of the charged lepton mixing matrix whereas the $\mu^+ \to e^+\gamma$ process is related to the off-diagonal terms. Models exist in which a prediction of the $\mu^+ \to e^+\gamma$ rate can be made as a function of the discrepancy of a_μ with respect to the SM value.[8] The present discrepancy is compatible with a possible $BR(\mu^+ \to e^+\gamma)$ in the range $10^{-13} \div 10^{-12}$.

1.2. *Historical perspective of the $\mu^+ \to e^+\gamma$ search*

The search for the $\mu^+ \to e^+\gamma$ decay started soon after the discovery of the μ-meson in the cosmic radiation (see Fig. 1). The first limit was set to less than 10% by Hinks and Pontecorvo in 1948[9] making use of cosmic ray muons. The limit improved constantly thanks to the development of pion beams first, and muon beams after the 1970s. The non-existence of this process at a level of 10^{-5} in the mid-1950s led directly to the two-neutrino hypothesis ($\nu_\mu \neq \nu_e$) which was verified a few years later.

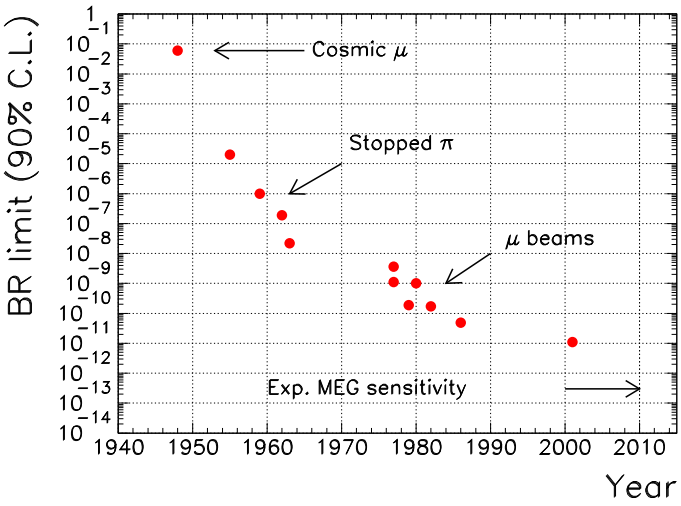

Fig. 1. Limit on the $\mu^+ \to e^+\gamma$ branching fraction as a function of the year. The expected sensitivity of the MEG experiment is also indicated.

Each improvement in the limit was linked to an improvement in beam or detector technology, and there has always been a trade-off between the various detector elements (*e.g.* efficiency versus resolution, solid angle versus time performance) to reach the optimal sensitivity.

The present experimental limit for the branching ratio $BR(\mu^+ \to e^+\gamma)$ is set by the MEGA experiment[10] to 1.2×10^{-11} and is one of the strongest bounds on the lepton-flavour number conservation.

2. Experimental search for the decay

The $\mu^+ \to e^+\gamma$ signal has a simple topology and appears as 2-body final state of a positron and a $\gamma-$ray, emitted in opposite directions with an energy of 52.8 MeV each, corresponding to half of the muon mass.

The background to such a measurement can be divided in "prompt" and "accidental" background. The former comes from radiative muon decays (RMD,

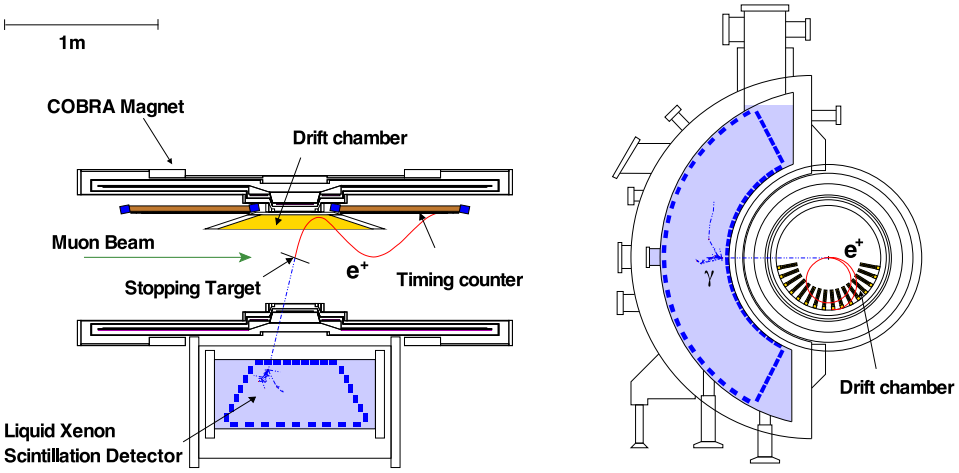

Fig. 2. Cross-sectional view of the MEG detector.

$\mu^+ \to e^+\nu\bar{\nu}\gamma$) in which the two neutrinos carry little energy, the latter comes from an accidental coincidence of a high energy positron from a normal (Michel) muon decay with an energetic photon coming from RMD, positron bremsstrahlung or annihilation in flight. It can be shown[11] that in experiments such as MEG, the accidental background dominates, and is proportional to the muon rate and the experimental resolutions on the particle kinematical variables:

$$BR_{\rm acc} \approx R_\mu \Delta E_{\rm e} \Delta E_\gamma^2 \Delta\theta_{\rm e\gamma}^2 \Delta t_{\rm e\gamma}. \quad (1)$$

The successful search for the $\mu^+ \to e^+\gamma$ decay needs therefore a detector with superior resolutions for both electrons and $\gamma-$rays at energies close to 52.8 MeV. The MEG experiment was designed to reach a sensitivity of few $\times 10^{-13}$, two orders of magnitude better than the present limit.

3. The MEG detector

The MEG detector schematics is depicted in Fig. 2. A high intensity beam of 28 MeV/c surface muons ($\sim 3 \times 10^7 \mu^+$/sec) is brought to rest in a thin polyethilene target. The positron four-momentum is measured by a magnetic spectrometer composed of a set of drift chambers immersed in a non-homogeneous magnetic field coupled to a plastic scintillator timing counter, that measures the positron emission time.

The $\gamma-$ray energy, conversion position and time are measured by an innovative liquid xenon calorimeter. Liquid xenon was chosen because of its short radiation lenght, high luminosity and fast scintillation signal.

3.1. *Beam line and target*

Secondary muons generated by the 590 MeV proton accelerator at PSI are captured by the $\pi E5$ beam line. A Wien filter deflects the positrons present in the beam in order to obtain a pure (better than percent) muon beam; the muons are focused by quadrupole triplets and through a superconducting transport solenoid (BTS), where a collimator is placed, reach the 205 μm CH_2 target placed at the center of the MEG spectrometer, in a beam spot with $\sigma_x \approx \sigma_y \approx 11$ mm.

3.2. *Positron spectrometer*

The MEG positron spectrometer COBRA (COnstant Bending RAdius) consists of a superconducting solenoidal magnet with the tracker inside, coupled to a fast timing system. The COBRA magnet changes radius along the z-axis and, as a result, its field changes from 1.27 Tesla at $z = 0$ and decreases as $|z|$ increases, reaching 0.49 Tesla at $z = 1.25$ m. In this way the positron are quickly swept away after being measured not to make the spectrometer blind. The gradient of the magnetic field was chosen such that positrons with the same absolute momenta follow trajectories with a constant transverse radius, independent of the emission angle. This allows a discrimination of high-momentum signal positrons from the Michel positrons originating from the target.

In order to keep the material budget as low as possible an open-frame construction for the drift chambers was adopted: the frames holding the anode and field wires have an opening on the side close to the muon stopping target; this allows positrons to be detected without scattering in the chamber frames. The frames themselves are made of a carbon fibre and are pre-tensioned before attaching the wires. The gas volume is closed by very thin foils, thus the amount of material in the fiducial volume due to the very light construction together with a use of He-C_2H_6 gas mixture, corresponds to only 1.5×10^{-3} radiation lenghts along the positron path. In total 16 radial drift chambers are placed inside the magnet. The $r-$coordinate of the track is determined by the drift time with a precision of ~ 230 μm. The cathodes are etched with a zig-zag shaped, 5 cm long periodic Vernier pattern therefore six signals are recorded for each chamber cell: two wire ends and four cathode signals. The rough $z-$coordinate is determined by the charge division at the wire ends, and refined by looking at the cathode charge asymmetry within the correct Vernier period. With this method a good $z-$resolution is obtained ($\sim 600 \div 700$ μm) keeping the chamber material as low as possible.

An array of plastic scintillators is placed on each side of the spectrometer to measure the e^+ emission time with a resolutions of 100 ps FWHM.

3.3. *The photon detector*

The γ-ray four-momentum is measured by a liquid xenon scintillation detector. This device consists of a single volume of liquid xenon viewed from all sides by about 800

photomultipliers (PMTs) immersed in the liquid at 165 K temperature. The total measured light gives an estimate of the photon energy while the light distribution on the front face is used to determine the position and time of its first interaction.

3.4. *Trigger and DAQ*

All the signals coming from the detector are processed by two waveform digitizers in parallel: a 2 GHz custom digitizer (DRS[12]) is used for offline analysis and its resolution is mandatory to search for possible pile-up effects. A 100 MHz FADC-based digitizer is used for trigger purposes: it receives the signals from the xenon detector, the timing counter and the drift chambers and performs an on-line computation of the photon energy and timing, positron direction and timing and their correlation. This reduces the rate from the initial $3 \times 10^7 \mu-$decays per second to an acquisition speed of 7 $\sec^{-1}$. The DRS chip is able to digitize 8+1 channels at a speed up to 6×10^9 samples per second with a resolution of 12 bits. The depth of each channel might be from 1024 bins and more, applying a cascading scheme. The analog bandwidth of the last version of the chip is extended up to 850 MHz which is enough even for the signals from the fast PMT. Custom-built VME boards have 4 DRS chips (total 32 channels) and an FPGA making a calibration and zero suppression in real time. It has been demonstrated that this solution allows the effective separation of pile-up events separated in time by less than 10 ns.

4. Calibrations

It is understood that in such a complex detector a lot of parameters must be constantly checked. For this reason there are redundant calibrations and monitoring tools regarding both single detectors (*e.g.* PMT equalization, inter-bar timing, energy scale) and multiple detectors simultaneously (relative timing). A list of some of these methods is presented in Tab. 1. As an example, for the xenon detector

Table 1. Typical calibrations that are performed to determine the liquid xenon detector performance (energy scale, linearity, etc.) together with their energy range and feasibility frequency.

Process		**Energy**	**Frequency**
Charge exchange	$\pi^- p \to \pi^0 n$ $\pi^0 \to \gamma\gamma$	55, 83, 129 MeV	year / month
Radiative $\mu-$decay	$\mu^+ \to e^+ \nu\bar{\nu}\gamma$	52.8 MeV endpoint	week
Proton accelerator	$^7\mathrm{Li}(p,\gamma_{17.6})^8\mathrm{Be}$	14.8, 17.6 MeV	week
	$^{11}\mathrm{B}(p,\gamma_{16.1})^{12}\mathrm{C}$	4.4, 11.6, 16.1 MeV	week
Nuclear reaction	$^{58}\mathrm{Ni}(n,\gamma_9)^{59}\mathrm{Ni}$	9 MeV	daily
Radioactive source	AmBe	4.4 MeV	daily

monitoring, several possibilities exist, which allow a survey of the detector in an

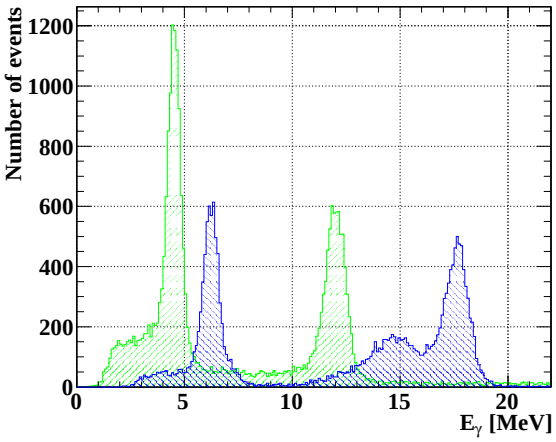

Fig. 3. Spectrum of $\gamma-$rays recorded by the liquid xenon detector coming from nuclear reactions induced by the MEG Cockcroft-Walton proton accelerator: $^{11}\mathrm{B}(p,\gamma_{4.4,11.6})^{12}\mathrm{C}$ (green) $^{7}\mathrm{Li}(p,\gamma_{17.6,14.8})^{8}\mathrm{Be}$ (blue).

energy range as large as possible:

(1) In the low energy region (5.5 MeV) α-source spots deposited on thin wires[13] are used to measure the PMT quantum efficiencies and the liquid xenon optical properties on a daily basis;
(2) In the intermediate energy region a Cockcroft-Walton accelerator is used, three times per week, to shoot protons, in the energy range 400-700 keV, against a $Li_2B_4O_7$ target. Photons of 17.6 MeV energy from $\mathrm{Li}(p,\gamma)\mathrm{Be}$ are used to monitor the xenon detector energy scale and resolution, while time coincident 4.4 MeV and 11.6 MeV photons from $\mathrm{B}(p,\gamma)\mathrm{C}$ are used to intercalibrate the timing of the xenon calorimeter with the positron timing counters (see Fig. 3).
(3) In the high energy region measurements of photons from π^0 decays from π^- charge exchange in a liquid hydrogen target are performed twice a year;
(4) LEDs and a custom developed LASER are used to monitor the stability of the subdetectors.

The possibility of having different ways of calibration and monitoring, complementary to each other, is of extreme importance for the experiment.

5. The 2008 run

In 2008 we had the first physics run after a short engineering run in 2007. During the summer of 2008 we proceeded with detector assembly, xenon purification and calibration of the detector (CEX runs). On 12 September we started data taking until 23 December. We ran for $\sim 7\times10^6$ s with an average live time of 50% (including

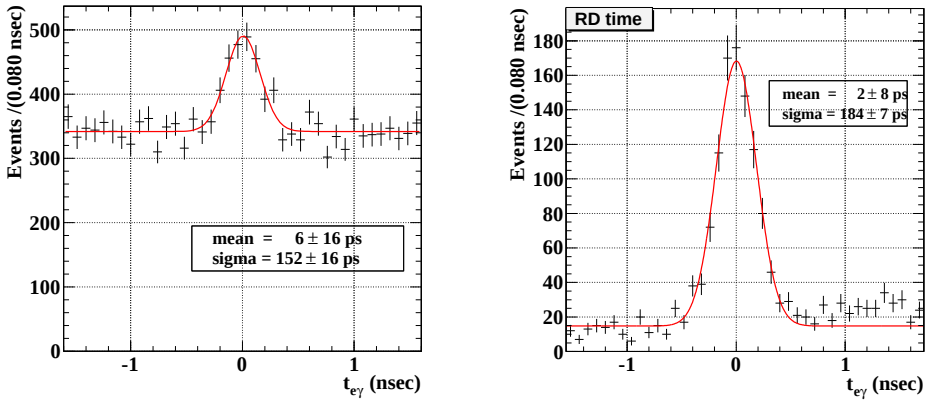

(*a*) (*b*)

Fig. 4. (*a*) Radiative peak in MEG. (*b*) Radiative peak in dedicated low intensity RMD runs. The E_γ and E_e thresholds were lower than in nominal physics runs and the back-to-back condition was released.

the machine weekly shut-down) corresponding to $\sim 10^{14}$ muon decays.

Once per week we had one day of data taking at reduced beam intensity to be able to see a clear RMD signal for calibration purposes. In Fig. 4 the time distribution of positron-γ coincidences is shown for normal (*a*) and reduced (*b*) beam intensities. The peak corresponding to radiative decay is clearly visible on top of the accidental background.

The 2008 run suffered from a severe problem of drift chamber (DCH) instability. An increasing number of chambers suffered frequent high-voltage failures and in the end we had to run at one-third of the nominal acceptance. The problem was solved during the 2009 shutdown, but influenced the statistics presented in this contribution.

6. Data analysis

The data collected in the 2008 run were used to perform a blind-box likelihood analysis. Events in which E_γ was close to 52.8 MeV and $t_{e\gamma} \sim 0$ were removed from the main data stream and hidden. Data in the sidebands were used to study the distribution of the kinematical variables, and to study the expected background in the signal region, since it is mainly due to accidental coincidences.

The probability density functions (*pdf*s) for the signal, RMD and accidental background were extracted from data, when possible, or from Monte Carlo computations using experimental inputs. For example the *pdf* for E_γ was extracted by a fit to the 55 MeV line of the π^0 decay in the CEX runs, scaled to 52.8 MeV. The E_e *pdf* was extracted by fitting a multi-component Gaussian resolution to the endpoint

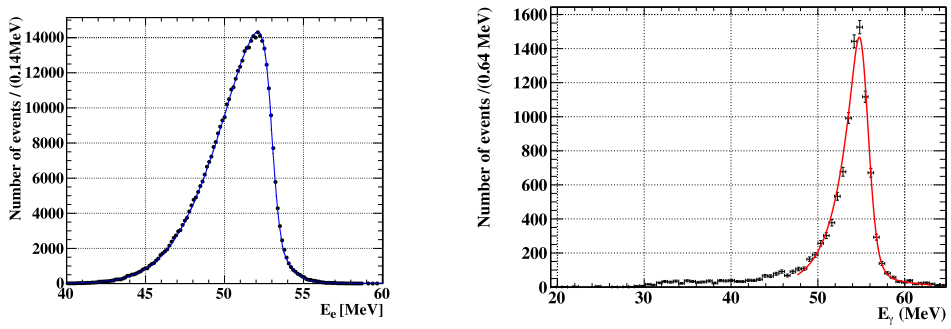

(a) (b)

Fig. 5. (a) Measured Michel positron energy spectrum. A solid line shows the fitted function as described in the text. (b) Measured energy spectrum for 54.9 MeV photons from a CEX run.

of the measured Michel spectrum (see Fig. 5).

The blinding-box was opened after completing the optimization of the analysis algorithms and the background study. The details of the analysis procedure and the discussion of the systematics is presented in reference.[14]

The number of $\mu^+ \to e^+\gamma$ events is determined by means of a maximum likelihood fit in the analysis window region defined as $46\,\mathrm{MeV} < E_\gamma < 60\,\mathrm{MeV}$, $50\,\mathrm{MeV} < E_\mathrm{e} < 56\,\mathrm{MeV}$, $|t_{e\gamma}| < 1\,\mathrm{ns}$, $|\theta_{e\gamma}| < 100\,\mathrm{mrad}$ and $|\phi_{e\gamma}| < 100\,\mathrm{mrad}$.

An extended likelihood function $\mathcal{L}$ is constructed as

$$\mathcal{L}(N_\mathrm{sig}, N_\mathrm{RMD}, N_\mathrm{BG}) = \frac{N^{N_\mathrm{obs}} e^{-N}}{N_\mathrm{obs}!} \prod_{i=1}^{N_\mathrm{obs}} \left[\frac{N_\mathrm{sig}}{N} S + \frac{N_\mathrm{RMD}}{N} R + \frac{N_\mathrm{BG}}{N} B \right],$$

where N_sig, N_RMD and N_BG are the number of $\mu^+ \to e^+\gamma$, RMD and accidental background (BG) events, respectively, while S, R and B are their probability density functions.

The 90 % confidence intervals on N_sig and N_RMD are determined by the Feldman-Cousins approach.[15] A contour of 90 % C.L. on the (N_sig, N_RMD)-plane is constructed by means of a toy Monte Carlo simulation. The obtained upper limit at 90 % C.L. is $N_\mathrm{sig} < 14.7$, where the systematic error is included. The largest contributions to the systematic error are from the uncertainty of the selection of photon pile-up events ($\Delta N_\mathrm{sig} = 1.2$), the response function of the positron energy ($\Delta N_\mathrm{sig} = 1.1$), the photon energy scale ($\Delta N_\mathrm{sig} = 0.4$) and the positron angular resolution ($\Delta N_\mathrm{sig} = 0.4$).

The upper limit on $\mathrm{BR}(\mu^+ \to e^+\gamma)$ is calculated by normalizing the upper limit on N_sig to the number of Michel positrons counted simultaneously with the signal and using the same analysis cuts, assuming $\mathrm{BR}(\mu \to e\nu\bar{\nu}) \approx 1$. This technique has the advantage of being independent of the instantaneous beam rate and is nearly insensitive to positron acceptance and efficiency factors associated with the DCH and

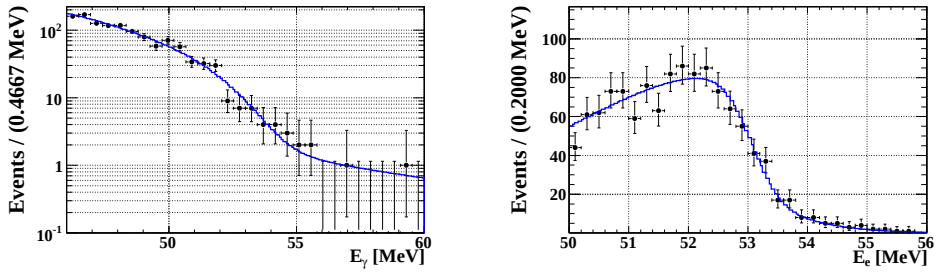

(a) (b)

Fig. 6. Projected distributions for $E_\gamma(a)$ and $E_e(b)$, containing all events in the analysis window. A solid line shows the likelihood functions fitted to the data.

TC detectors. These differ only slightly between the signal and the normalization samples, due to small momentum dependent effects.[14]

The limit on the branching ratio of the $\mu^+ \to e^+\gamma$ decay is[a]

$$\mathrm{BR}(\mu^+ \to e^+\gamma) \leq 2.8 \times 10^{-11} \qquad (90\%\mathrm{C.L.})$$

where the systematic uncertainty on the normalization is taken into account.

The upper limit can be compared with the branching ratio sensitivity of the experiment with these data statistics. This is defined as the average upper limit of the branching ratio, extracted with toy Monte Carlo simulations, assuming a null signal and the same numbers of accidental background and RMD events as in the data.[15] The branching ratio sensitivity in this case is estimated to be 1.3×10^{-11}, which is comparable with the current branching ratio limit set by the MEGA experiment.[10] Given this branching ratio sensitivity, the probability to obtain the upper limit greater than 2.8×10^{-11} is ~ 5 % if systematic uncertainties in the analysis are taken into account.

7. Status and perspectives

After a start-up engineering run in 2007 we had the the first MEG physics run at the end of 2008, which suffered from detector instabilities. Data from the first three months of operation of the MEG experiment give a result which is competitive with the previous limit.

During 2009 shutdown the problem with the drift chamber instability was solved and the detector operated for all the 2009 run with no degradation. We had physics data taking in November and December 2009 with improved efficiency, improved electronics and improved resolutions. We are confident in obtaining a sensitivity that should allow us to improve the present experimental limit.

[a]At the conference a slightly worse limit was shown, namely $\mathrm{BR}(\mu^+ \to e^+\gamma) \leq 3.0 \times 10^{-11}$. In the meanwhile a better estimate of the systematic uncertainty was performed. The result reported here is consistent with the one published in.[14]

The experiment is scheduled to run until the end of 2011 to reach the target sensitivity of the experiment.

Acknowledgments

I want to thank the organizer of the BEYOND2010 conference for the perfect organization and for giving me the opportunity of visiting the wonderful city of Cape Town. I met many colleagues from all around the world with whome I had pleasant discussions, not only regarding physics. The walk to the top of Table Mountain with Dr. Z. Ahmed, Dr. S. Capelli, Dr. D. D'Angelo and Dr. C. Kiessig was memorable!

References

1. A. Baldini, T. Mori *et al.*, "The MEG experiment: search for the $\mu \to e\gamma$ decay at PSI", available at `http://meg.psi.ch/docs`
2. R. Barbieri *et al.*, Nucl. Phys. B **445** (1995) 225
3. J. Hisano *et al.*, Phys. Lett. B **391** (1997) 341
4. A. Masiero *et al.*, Nucl. Phys. B **649** (2003) 189
5. T. Schwetz, M. A. Tortola and J. W. F. Valle, New J. Phys. **10** (2008) 113011. A. Strumia and F. Vissani, `arXiv:hep-ph/0606054v3`
6. L. Calibbi *et al.*, Phys. Rev. D **74** (2006) 116002
7. C. Amsler *et al.* [Particle Data Group], Phys. Lett. **B**667 (2008) 1 (pag. 481-482)
8. G. Isidori *et al.*, Phys. Rev. D **75** (2007) 115019
9. E. P. Hincks and B. Pontecorvo, Can. J. Res. **28A**, 29 (1950), reprinted in S. M. Bilenky *et al.* (editors) "Bruno Pontecorvo" Società Italiana di Fisica (1997)
10. M. L. Brooks *et al.* [MEGA Collaboration], Phys. Rev. Lett. **83**, (1999) 1521.
11. Y. Kuno and Y. Okada, Rev. Mod. Phys. **73** (2001) 151.
12. S. Ritt, Nucl. Instrum. Meth. A **518**, 470 (2004).
13. A. Baldini *et al.*, Nucl. Instrum. Meth. A **565**, 589 (2006).
14. J. Adam *et al.* [MEG Collaboration], Nucl. Phys. B **834**, (2010) 1.
15. G. J. Feldman and R. D. Cousins, Phys. Rev D **57**, (1998) 3873.